Malaysian Simulation SOCIETY
http://amsjournal.ams-mss.org
APPLICATIONS OF MODELLING AND SIMULATION
eISSN 2600-8084
VOL 2, NO. 2, 2018, 59-69

A Chattering Suppression of Proportional Sliding Mode Control with Composite Nonlinear Feedback Technique using Sigmoid Function for MacPherson Active Suspension System

M. Fahezal Ismail[1*], Yahaya Md. Sam[2], S. Sudin[2], K. Peng[3] and M. Khairi Aripin[4]

[1]Industrial Automation Section, Universiti Kuala Lumpur Malaysia France Institute, Section 14 Jalan Teras Jernang 43650 Bandar Baru Bangi, Selangor, Malaysia.
[2]School of Electrical Engineering, Universiti Teknologi Malaysia, 81310 UTM Skudai, Johor, Malaysia.
[3]Temasek Laboratories, National University of Singapore, 5A, Engineering Drive 1, Singapore 117411, Singapore.
[4]Faculty of Electrical Engineering, Universiti Teknikal Malaysia Melaka, Hang Tuah Jaya, 76100 Durian Tunggal, Melaka, Malaysia

[*]Corresponding author: fahezal@unikl.edu.my

Abstract: The chattering problem phenomenon occurred due to the high-frequency switching of a sliding mode controller exciting unmodelled dynamics in the closed loop. Unmodelled dynamics may be those of sensors and actuators neglected in the principal modelling process since they are generally significantly faster than the main system dynamics. In the MacPherson active suspension system, the phenomenon occurred due to unmodelled dynamics on tire in a quarter car model. The Proportional Integral Sliding Mode Control (PISMC) is combined with Composite Nonlinear Feedback (CNF) technique due to its characteristics on the transient response and fast settling time. The sigmoid function is used in PISMC-CNF control law to reduce chattering problem. The Evolution Strategy is used to find the best boundary layer thickness based on the road profiles applied to the MacPherson active suspension system. The results show the significant of the proposed solution in the mentioned application based on acceleration of spring mass.

Keywords: Boundary layer solution; Chattering problem; Sigmoid function; Unmodelled dynamics.

1. INTRODUCTION

The MacPherson car suspension system uses the axis of a telescopic damper as the upper steering pivot. Earle S. MacPherson developed the design of the strut in 1949. It has become one of the most widely used designs in the vehicle suspension system in modern automotive design. To facilitate the ideal suspension with regard to comfort, handling, and safety, various commercial technologies have been used to improve or replace the conventional passive suspension system.

In the modern automotive active suspension modelling, there are three mathematical models used by the researchers in the past research work [1]. The quarter car model consists of two degrees of freedom (DOF) for the vertical dynamic equation including sprung mass and unsprung mass. A half-car model consists of four DOF of the vertical dynamic equation which represents either the vertical and pitch motions corresponding to the bicycle model or the vertical and roll motions corresponding to the axle model. A full car model consist of seven DOF including roll, pitch, vertical motions of wheels and vertical motions of the vehicle body. The quarter car model active suspension system is the most popular model for control performance in ride comfort and road handling quality due to its simplicity but significant.

The MacPherson model is usually used as front suspension of the vehicle and also can be used for both front and rear suspensions. Hong et al. [2] focused on the new modelling of MacPherson active suspension system that is the rotational motion of the unsprung mass. The two generalised coordinates selected in this new model were the vertical displacement of the sprung mass and the angular displacement of the control arm. The authors claimed that the new model was more general in the sense that it provided an extra degree of freedom in determining a plant model for control system design. However the authors did not mention about self-steer phenomenon. Chen and Beale [3] claimed that the motion equation was successfully derived with off-the-centre-of-mass of body-fixed coordinates in Euler parameters. This research work puts the foundation for experimental measurements of base dynamic parameters and the application of base dynamic parameter estimation techniques in suspension design. A study about uncertainties in the MacPherson suspension system is an important issue to propose a control strategy to the system. However, the authors did not mention any control strategy to apply in the MacPherson active suspension system.

Goh et al. [4] presented a case study of a MacPherson automotive suspension analysis, and evaluated the uncertainties in the modelling of this complex dynamic problem, using a simplified analytical model and a complex computational model. However, the finding of this research was to identify the uncertainty in the suspension system used and did not mention about self-steer. Hurel et al. [5] proposed kinematic-dynamic model for the MacPherson active suspension system. They also proposed a systematic development of the planar model as well as the complete set of mathematical equations. The proposed model has been compared to a realistic Adams/View model to analyse dynamic behaviour against road perturbations and two relevant kinematic parameters: camber angle and track width variation.

The first step of Variable Structure Control Systems was invented from the ground-breaking work in Russia by Emel'yanov and Barbashin in the early 1960s. The concept was used in Russia until the mid of 1970s when a book by Itkis and a review paper by Utkin were published in English version in 1976 and 1977 respectively. The control strategies have been applied in the design of robust controller, model-reference systems, adaptive control, tracking systems, state observes and fault detection control. The Sliding Mode Control (SMC) is widely used in various engineering fields. Sam et al. [6] used PISMC in a linear quarter car model active suspension system. Lin and Lian [7] used ISMC in a full car active suspension system, whereas Chamseddine et al. [8] used SMC in a linear full car active suspension system. Zhou and Zhang [9] and Chen et al. [10] used SMC in a semi-active suspension system. Pati et al. [11] used SMC in a half-car model active suspension system, while Puleston et al. [12] and Xiaoqiu and Yurkovich [13] used SMC for speed control in an automotive engine. Govindaswamy et al. [14] and Alwi and Edward [15] used SMC controller to control the lateral dynamics of the F-14 aircraft under powered approach.

Zhang and Lan [16] used Composite Nonlinear Feedback (CNF) for control of a DC motor in a hard drive with fast response and reduced overshoot by varying the damping ratio. Moreover, Lin et al. [17] described the concept of CNF for tracking control performance for linear system. It was the best reference for understanding the CNF controller design. The authors claimed that the designed nonlinear feedback law causes the output to track a high amplitude step input rapidly without experiencing a large overshoot, as well as, without the adverse actuator saturation effects. On the other hand, Chen et al. [18] studied the theory and the applications of the CNF. It was an expanded research work from [17]. The authors classified the CNF in three cases, i.e., the state feedback, the full order measurement feedback, and the reduced-order measurement cases. The details of derivation and proof were given as well. This rest of the paper is organised as follows Section 2 presents system modelling of a quarter car active suspension system. Section 3 elaborates the controller design of PISMC-CNF based on a MacPherson active suspensions. Section 4 gives results and analysis based on the boundary layer thickness and sigmoid function and finally Section 5 gives a conclusion of the research work.

2. SYSTEM MODELLING

2.1 Quarter Car Model of MacPherson Active Suspension System

The quarter car model for MacPherson active suspension system uses the Lagrange equation. As shown in Figure 1, let (Y_A, Z_A), (Y_B, Z_B) and (Y_C, Z_C) denote the coordinates of points *A*, *B* and *C*, respectively, when the suspension system is at an equilibrium point. Then, the following equations hold:

$$Y_A = 0 \tag{1}$$

$$Z_A = Z_s \tag{2}$$

$$Y_B = l_B(\cos(\theta - \theta_0) - \cos(-\theta_0)) \tag{3}$$

$$Y_B = Z_s + l_B(\sin(\theta - \theta_0) - \sin(-\theta_0)) \tag{4}$$

$$Y_C = l_C(\cos(\theta - \theta_0) - \cos(-\theta_0)) \tag{5}$$

$$Y_C = Z_s + l_C(\sin(\theta - \theta_0) - \sin(-\theta_0)) \tag{6}$$

where θ_0 is the initial angular displacement of the control arm at an equilibrium point.

Let $\alpha' = \alpha + \theta_0$. Then, the following relations are obtained from the triangle *OAB*.

$$l = (l_A^2 + l_B^2 - 2l_A l_B \cos\ \alpha')^{1/2} \tag{7}$$

$$l' = (l_A^2 + l_B^2 - 2l_A l_B \cos\ \alpha' - \theta)^{1/2} \tag{8}$$

where l is the initial distance from *A* to *B* at an equilibrium state, and l' is the changed distance from *A* to *B* with the rotation of the control arm by θ. Therefore, the deflection of the spring, relative velocity of the damper and deflection of the tyre are:

$$(\Delta l)^2 = (l - l')^2 = 2a_l - b_l(\cos\alpha' + \cos(\alpha' - \theta)) - 2\{a_l^2 - a_l b_l(\cos\alpha' + \cos(\alpha' - \theta) + b_l^2 \cos\alpha' \cos(\alpha' - \theta))\}^{\frac{1}{2}} \tag{9}$$

$$\dot{\Delta l} = \dot{l} - \dot{l}' = \frac{b_l \sin(\alpha' - \theta)\dot{\theta}}{2(a_l - b_l \cos(\alpha' - \theta))^{1/2}} \tag{10}$$

$$Z_C - Z_r = l_C(\sin(\theta - \theta_0) - \sin(-\theta_0)) - Z_r \tag{11}$$

where $a_l = l_A^2 + l_B^2$ and $b_l = 2l_A l_B$.

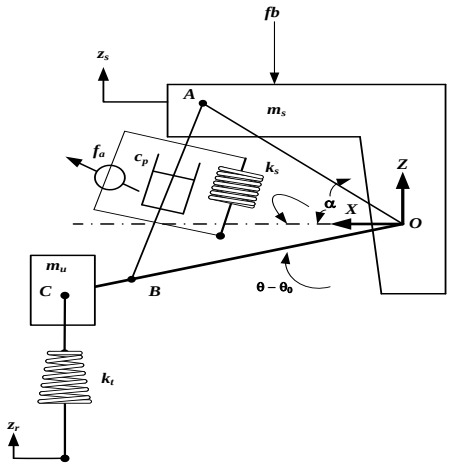

Figure 1. A free body diagram of quarter car model of the MacPherson active suspension system [2]

The equations of motion of the new model are now derived by the Lagrangian mechanics. Let *T*, *V* and *D* denote the kinetic, potential and the damping energies of the system, respectively. Then the equations are:

$$T = \frac{1}{2}m_s\dot{Z}_s^2 + \frac{1}{2}m_u\left(\dot{Y}_C^2 + \dot{Z}_C^2\right) \tag{12}$$

$$V = \frac{1}{2}k_s(\Delta l)^2 + \frac{1}{2}k_t(Z_C - Z_r)^2 \tag{13}$$

$$D = \frac{1}{2}c_p\left(\dot{\Delta}l\right)^2 \tag{14}$$

Substituting the derivatives of Equations (5), (6), (9), (10) and (11) into Equations (12), (13) and (14) yields

$$T = \frac{1}{2}(m_s + m_u)\dot{Z}_s^2 + \frac{1}{2}m_u l_C^2\dot{\theta}^2 + m_u l_C\cos\theta\,\dot{\theta}\dot{Z}_s \tag{15}$$

$$V = \frac{1}{2}k_s\left[2a_l - b_l(\cos\alpha' + \cos(\alpha' - \theta)) - 2\{a_l^2 - a_l b_l(\cos\alpha' + \cos(\alpha' - \theta) + b_l^2\cos\alpha'\cos(\alpha' - \theta))\}^{\frac{1}{2}}\right]^2 + \frac{1}{2}k_t[Z_s + l_C(\sin(\theta - \theta_0) - \sin(-\theta_0)) - Z_r]^2 \tag{16}$$

$$D = \frac{c_p b_l^2\sin^2(\alpha' - \theta)\dot{\theta}}{8(a_l - b_l\cos(\alpha' - \theta))} \tag{17}$$

Finally, for the two generalised coordinates, $q_1 = Z_s$ and $q_2 = \theta$ the motion equation for a quarter car model of the MacPherson active suspension system in Figure 1 can be represented as [2]:

The first Lagrange equation of motion yields

$$(m_s + m_u)\ddot{Z}_s + m_u l_C\cos(\theta - \theta_0)\,\ddot{\theta} - m_u l_C\sin(\theta - \theta_0)\,\dot{\theta}^2 + k_t(z_s + l_C(\sin(\theta - \theta_0)) - \sin(\theta_0) - Z_r) = -f_b \tag{18}$$

The second Lagrange equation of motion gives

$$m_u l_C^2\ddot{\theta} + m_u l_C\cos(\theta - \theta_0)\,\ddot{Z}_s + \frac{c_p b_l^2\sin(\alpha' - \theta_0)\dot{\theta}}{4(a_l - b_l\cos(\alpha' - \theta))} + k_t l_C\cos(\theta - \theta_0)(Z_s + l_C(\sin(\theta - \theta_0) - \sin(-\theta_0)) - Z_r) - \frac{1}{2}k_s\sin(\alpha' - \theta)\left[b_l + \frac{d_l}{\left(c_l - d_l\cos(\alpha' - \theta)^{1/2}\right)}\right]\dot{Z}_s = -l_B \tag{19}$$

where $c_l = a_l^2 - a_l b_l\cos(\alpha + \theta_0)$ and $d_l = a_l b_l - b_l^2\cos(\alpha + \theta_0)$.

The nomenclatures are m_s= mass of the car body (kg), m_u= mass of the car wheel (kg), k_s= stiffness of the car body spring (N/m), k_t= stiffness of car tyre (N/m), c_p= damper coefficient (Ns/m), l_A= distance from point 0 to *A*, l_B= distance from point 0 to *B*, l_C= distance from point 0 to *C*, f_b= weight of human body, f_a= actuator force, Z_s= displacement of sprung mass, $\dot{Z}_s$= velocity of sprung mass, $\ddot{Z}_s$= acceleration of sprung mass, θ_0= initial angular displacement of control arm, θ= angular displacement of control arm, $\dot{\theta}$= angular velocity of control arm, $\ddot{\theta}$= angular acceleration of control arm, Z_r= displacement of road profile, c_{p1}= the linear damping coefficient, c_{p2}= the nonlinearity damping coefficient, k_{s1}= the linear stiffness of car body spring, k_{s2}= the nonlinearity stiffness of car body spring, Δm_s= the uncertainty of sprung mass, Δk_t= the uncertainty of

stiffness of car tyre, Δc_{p1}= the uncertainty of linear damping coefficient, Δc_{p2}= the uncertainty of nonlinearity damping coefficient, Δk_{s1}= the uncertainty of linear stiffness of car body spring and Δk_{s2}= the uncertainty of nonlinearity stiffness of car body spring. Table 1 shows the detail parameters used in the mathematical modelling of a MacPherson model based on [1-2] as:

Table 1. Parameter values for the MacPherson active suspension quarter car model in [1]

Parameter	Value
Mass of a car body, $\boldsymbol{m_s}$	455 kg
Mass of a car wheel, $\boldsymbol{m_u}$	71 kg
Stiffness of a car body spring, $\boldsymbol{k_s}$	17,659 N/m
Stiffness of a car tyre, $\boldsymbol{k_t}$	183,888 N/m
Damper coefficient, $\boldsymbol{c_p}$	1950 Ns/m
Distance from point 0 to *A*, $\boldsymbol{l_A}$	0.37 m
Distance from point 0 to *B*, $\boldsymbol{l_B}$	0.64 m
Distance from point 0 to *C*, $\boldsymbol{l_C}$	0.66 m
Weight of human body, $\boldsymbol{f_b}$	80 kg

3. CONTROLLER DESIGN

The controller design is based on Proportional Integral Sliding Mode Control with Composite Nonlinear Feedback technique (PISMC-CNF) due to the capabilities to reduce the angular acceleration of control arm to get good road handling. On the other hand the PISMC-CNF can also reduce the acceleration of sprung mass to give the best performance of ride comfort.

3.1 PISMC-CNF

The main characteristic in designing the sliding mode control is that the control input must be designed to achieve the reaching condition $\sigma_{qMP}(t)\dot{\sigma}_{qMP}(t) < 0$. The proposed controller applied to the MacPherson active suspension system can be written as follows:

$$u_{PISMC-CNF}(t) = u_{qMPeq}(t) + u_{qMPs}(t) \tag{20}$$

The equivalent control $u_{qMPeq}(t)$ is designed. The switching control $u_{qMPs}(t)$ is applied as follows:

$$u_{qMPs}(t) = \left(\left(C_{qMP}B_{qMP}\right)^{-1}\sigma_{qMP}(t)\right) = \begin{cases} 1\ for\left(\left(C_{qMP}B_{qMP}\right)^{-1}\sigma_{qMP}(t)\right) > 0, \\ 0\ for\ \left(\left(C_{qMP}B_{qMP}\right)^{-1}\sigma_{qMP}(t)\right) = 0, \\ -1\ for\ \left(\left(C_{qMP}B_{qMP}\right)^{-1}\sigma_{qMP}(t)\right) < 0. \end{cases} \tag{21}$$

The expression in Equation (21) is usually written more concisely as:

$$u_{qMPs}(t) = -\varphi_1 sign\left(\left(C_{qMP}B_{qMP}\right)^{-1}\sigma_{qMP}(t)\right) \tag{22}$$

From Equation (22), the φ_1 is sliding gain. The switching control $u_{qMPs}(t)$ is clearly discontinuous and the $sign\left(\left(C_{qMP}B_{qMP}\right)^{-1}\sigma_{qMP}(t)\right)$ function is the will caused by the chattering problem [19]. Therefore, a control strategy is designed to ensure that the system dynamic is approximated to $\sigma_{qMP}(t)$ and nearly achieve to the ideal sliding mode dynamics. Moreover, in order to reduce the chattering problem, the boundary layer with sigmoid function continuous control law is proposed for the nonlinear switching control component, as given the following:

$$u_{qMPs}(t) = -\omega - \varphi_1 \frac{\left(\left(C_{qMP}B_{qMP}\right)^{-1}\sigma(x,t)\right)}{\left\|\left(\left(C_{qMP}B_{qMP}\right)^{-1}\sigma(x,t)\right)\right\| + \mu} \tag{23}$$

where $\omega = (\,f(x,\delta,t) + fx(t))$, μ is boundary thickness that is chosen to reduce chattering problem, and $\varphi_1$is sliding gain. Both parameters are very significant to the MacPherson active suspension system. If the value of μ is small, the control input will have high switching gain and would not display the capability of reducing a chattering problem. Figure 2 shows the effect of μ in the control components of both discontinuous and continuous.

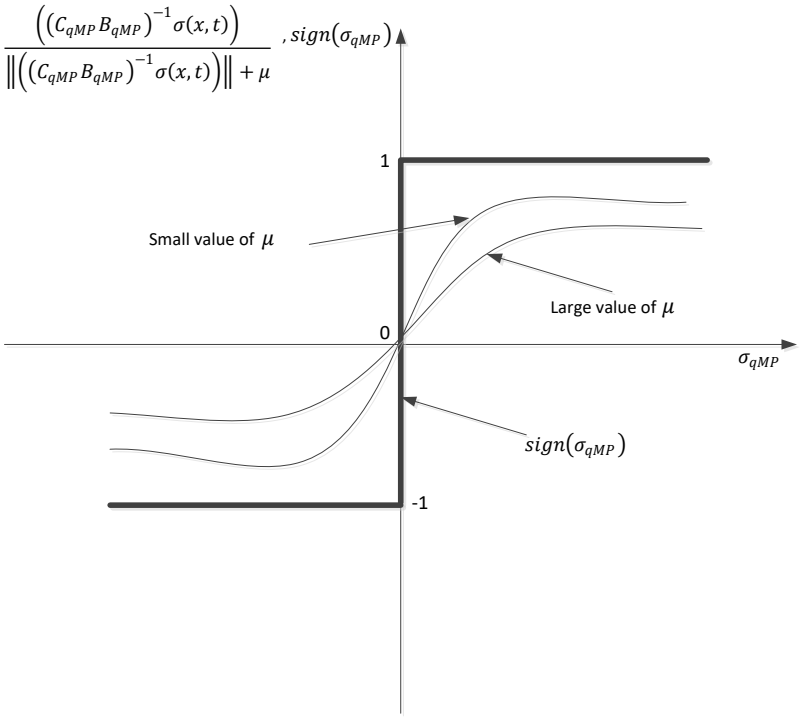

Figure 2. The effect of μ in the sigmoid function for discontinuous and continuous systems

A complete block diagram of the proposed PISMC-CNF controller used to control the MacPherson active suspension system is illustrated in Figure 3. Three types of road profiles were employed in these numerical simulation, where their functions as a disturbance to the system as shown from Figures 4-6. Under these road profiles, the control performance was validated. Most of the simulations carried out were based on the properties of the PISMC-CNF.

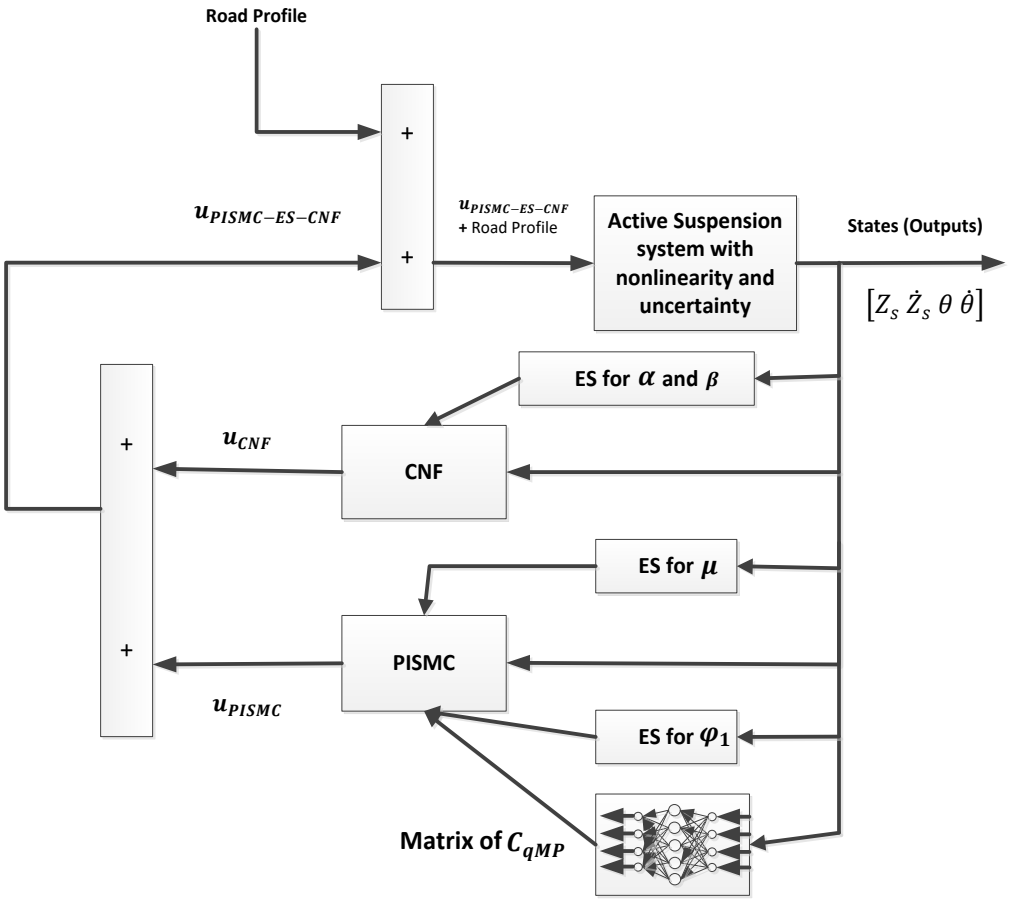

Figure 3. A block diagram of the PISMC-CNF controller for MacPherson active suspension system

4. RESULTS AND DISCUSSION

The results were obtained based on the numerical simulations of boundary layer thickness and sigmoid function. The purposes of MacPherson active suspension control design are to reduce vertical acceleration of sprung mass for ride comfort quality, to control the control arm for road handling performance, and to limit the acceleration of sprung mass not more than 0.315 m/s^2 based on the ISO 2631-1, 1997 as shown in Table 2 [20].

Table 2. Vertical acceleration for sprung mass level and degree of comfort (ISO2631-1, 1997)

RMS vertical acceleration level	Degree of comfort
(1) Less than 0.315 m/s^2	Not uncomfortable
(2) 0.315-0.63 m/s^2	A little uncomfortable
(3) 0.5-1 m/s^2	Fairly uncomfortable
(4) 0.8-1.6 m/s^2	Uncomfortable
(5) 1.25-2.5 m/s^2	Very uncomfortable
(6) Greater than 2 m/s^2	Extremely uncomfortable

Three road profiles as shown in Figures 4-6 were used in these numerical simulations in order to test the control performance in MacPherson active suspension system.

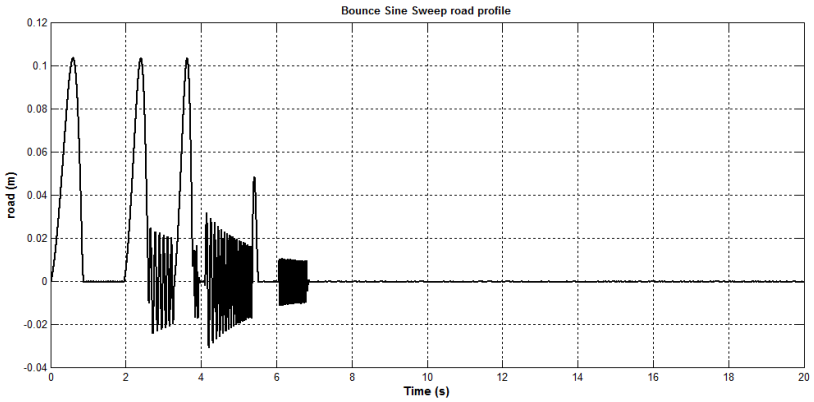

Figure 4. Bounce sine sweep road profile

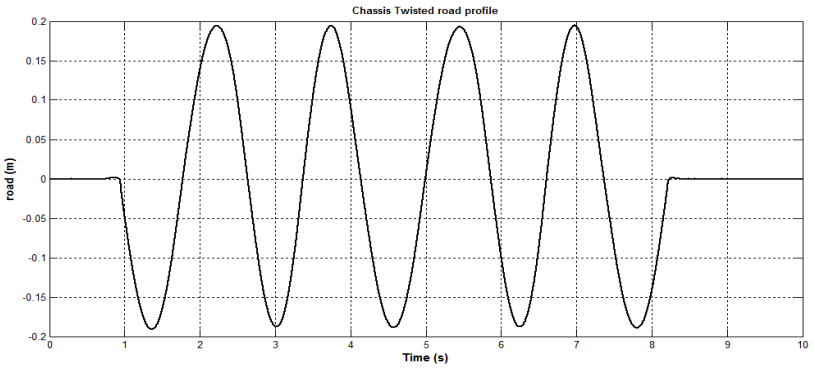

Figure 5. Chassis twisted road profile

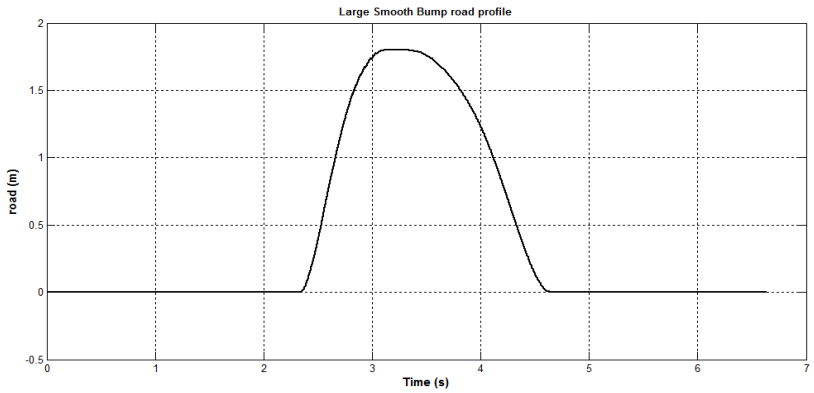

Figure 6. Large smooth bump road profile

4.1 Boundary Layer Thickness

The Evolutionary Strategy that had been engaged to search the best value of μ_1 and μ_2 is shown in Figure 7. The boundary layer is important to reduce the chattering problem in the PISMC-CNF controller.

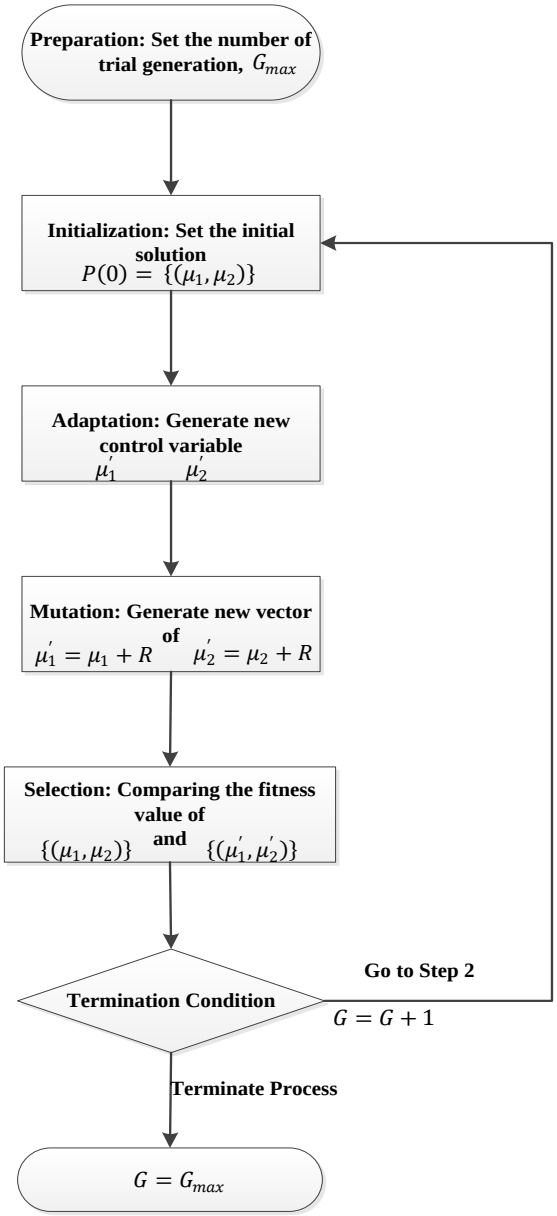

Figure 7. An algorithm for searching the value of boundary layer thickness

Under this numerical experiment procedure, the effect of boundary layer thickness was tested under three different road profiles. The two best values of μ_1 and μ_2 were as shown in Table 3.

Table 3. Boundary layer thickness in three different road profiles

	μ_1	μ_2
Bounce Sine Sweep	11.2344	0.1673
Chassis Twisted	11.9683	0.1545
Large Smooth Bump	12.1436	0.1422

The μ_2 parameter affects the MacPherson active suspension by having a very high chattering problem. Figures 8(a) to 8(c) show that μ_1 gave a good response in terms of reducing chattering for acceleration of sprung mass. The proposed control strategy showed that it successfully achieved a degree of comfort as mentioned in Table 2. The results obtained also proved that μ_1 reduced the chattering problem that occurred in the PISMC-CNF control law.

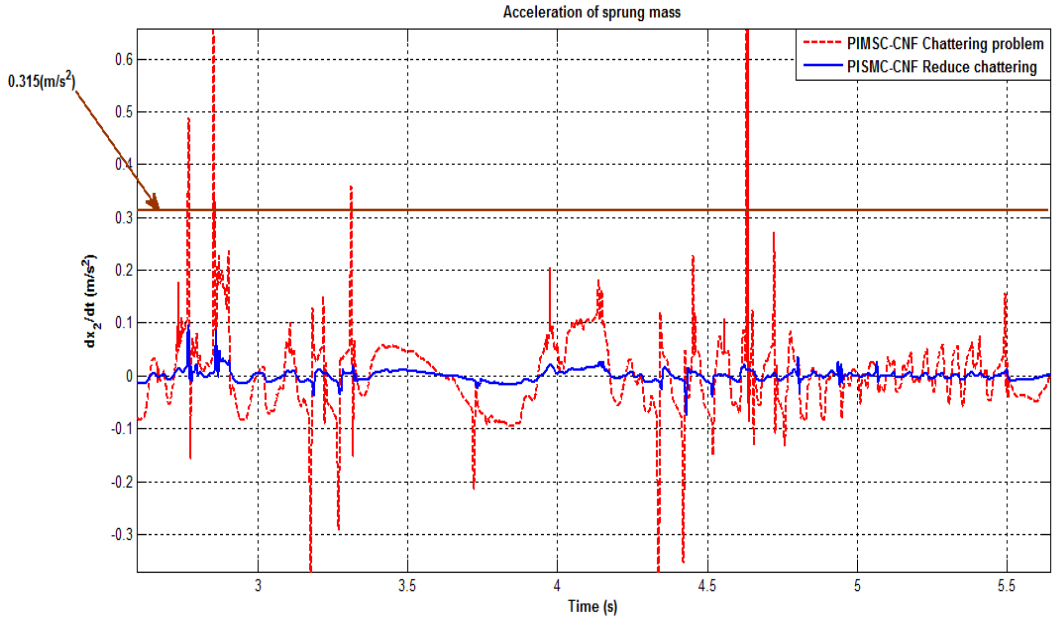

(a)

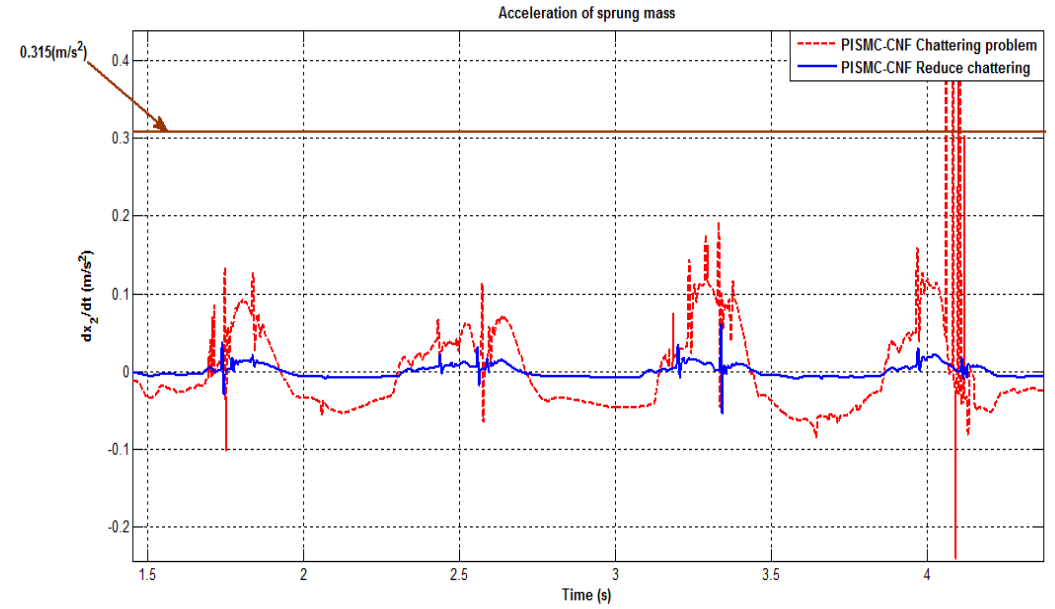

(b)

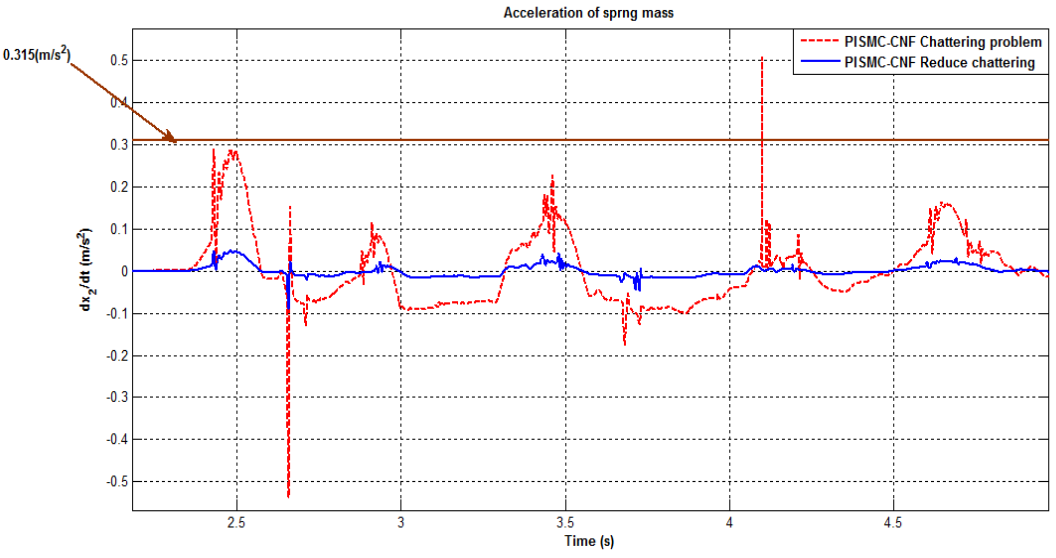

(c)

Figure 8. Acceleration of sprung mass effect for: (a) Bounce sine sweep (b) Chassis twisted and (c) Large smooth bump

4.2 Sigmoid Function

The sigmoid function cases were applied in this numerical simulations for control performance since Mobayen [21-25] and Bandyopadhyay [26] used in ISMC-CNF. The difference between ISMC and PISMC are at the function of controller of integral factor and proportional factor. The integral factor gives the zero steady state error while the proportional factor affects the transient performance. However, the ISMC is only suitable for matched uncertainties but on contrary, an active suspension system is unmatched uncertainties for road disturbances (road profiles). Therefore the PISMC was introduced in order to overcome the unmatched uncertainties condition. Table 4 compares the control strategies between PISMC-CNF and ISMC-CNF in details.

Table 4. Comparison of control strategies (control law) using PISMC/ISMC-CNF

From [22] and [23]	Proposed PISMC-CNF	From [26]
Sigmoid function	**Sigmoid function**	**Sigmoid function**
$u_{ISMC}(t)$ $= \begin{cases} u_{CNF} - \rho(x,t)\dfrac{(CB)^T s}{\|(CB)^T s\|}, \\ if\ s \neq 0 \\ u_{CNF}, if\ s = 0 \end{cases}$ where $\rho(x,t)$ is the switching function	$u_{PISMC}(t)$ $= \omega - \varphi_1 \dfrac{\left(\left(C_{qMP}B_{qMP}\right)^{-1}\sigma(x,t)\right)}{\left\|\left(\left(C_{qMP}B_{qMP}\right)^{-1}\sigma(x,t)\right)\right\| + \mu}$ where $\omega = (\Delta f(x,\delta,t) + fx(t))$ φ_1 is sliding gain μ is boundary layer thickness	$u_{ISMC}(t)$ $= -\eta\|s\|^{\alpha_1}\dfrac{((GB)^T s(x,t))}{\|(GB)^T s(x,t)\| + \theta_{ss}}$ where θ_{ss} is small which decides a width of band of the sliding surface. η is a reachability condition. α_1 is a controller parameter.

The comparison study was done between ISMC-CNF in [22-23], ISMC-CNF in [26] and the proposed controller PISMC-CNF. The numerical simulation procedure was based on the three different road profiles. Figure 9 shows that the PISMC-CNF controller exhibited a good transient performance, reduced overshoot, zero steady state error and fast response in displacement, as well as velocity of sprung mass. Nevertheless, the results using the ISMC-CNF [22-23], and the ISMC-CNF [26] showed a high chattering problem. Based on Table 2, ride comfort degree of vertical acceleration of the sprung mass level was less than 0.315 m/s^2. Therefore the controllers satisfied the ISO 2631-1, 1997 standard level of ride comfort as a not uncomfortable (the best ride comfort).

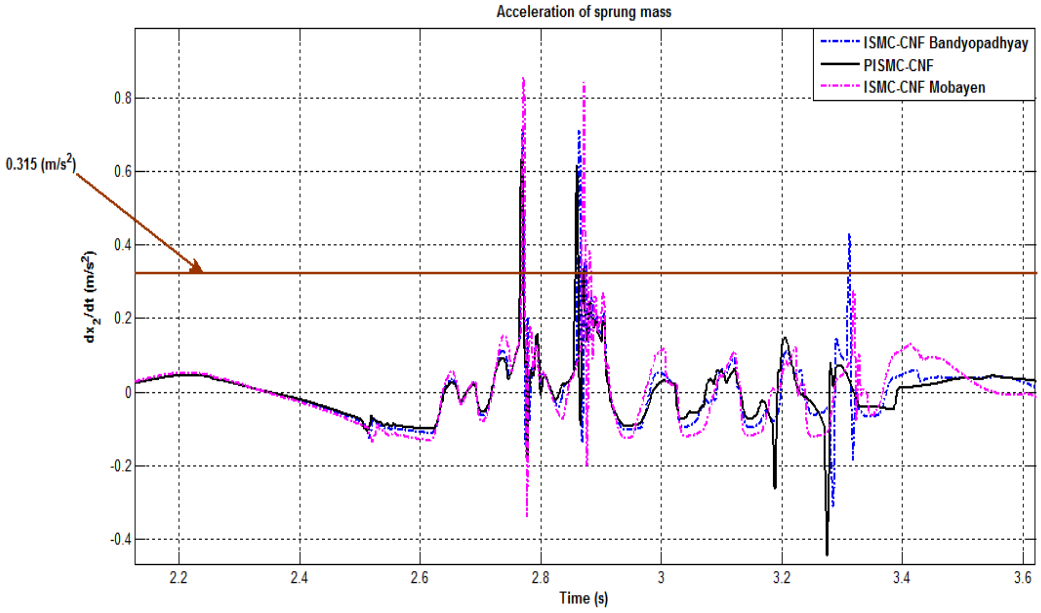

(a)

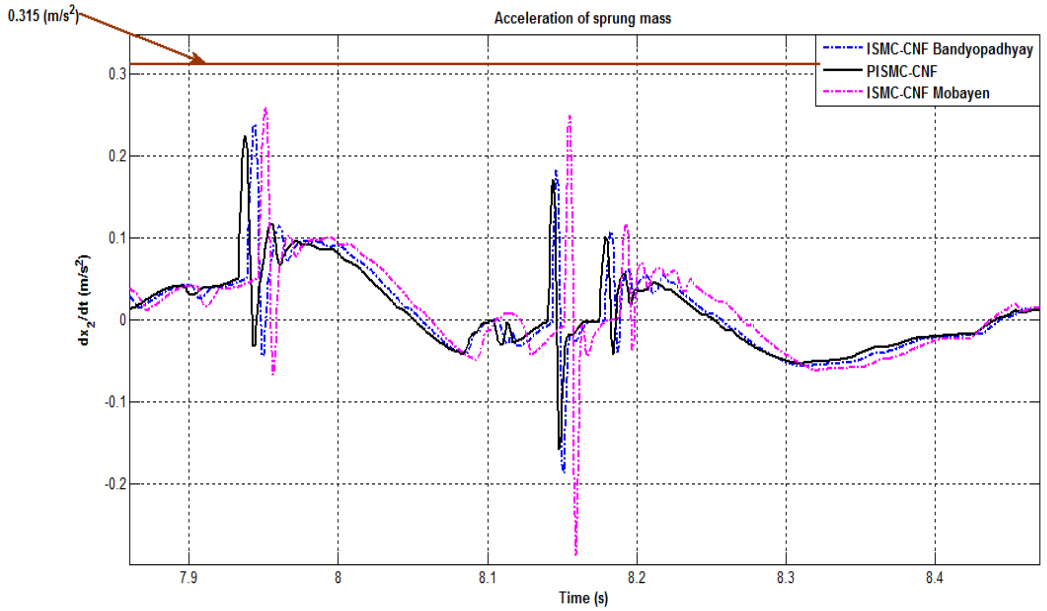

(b)

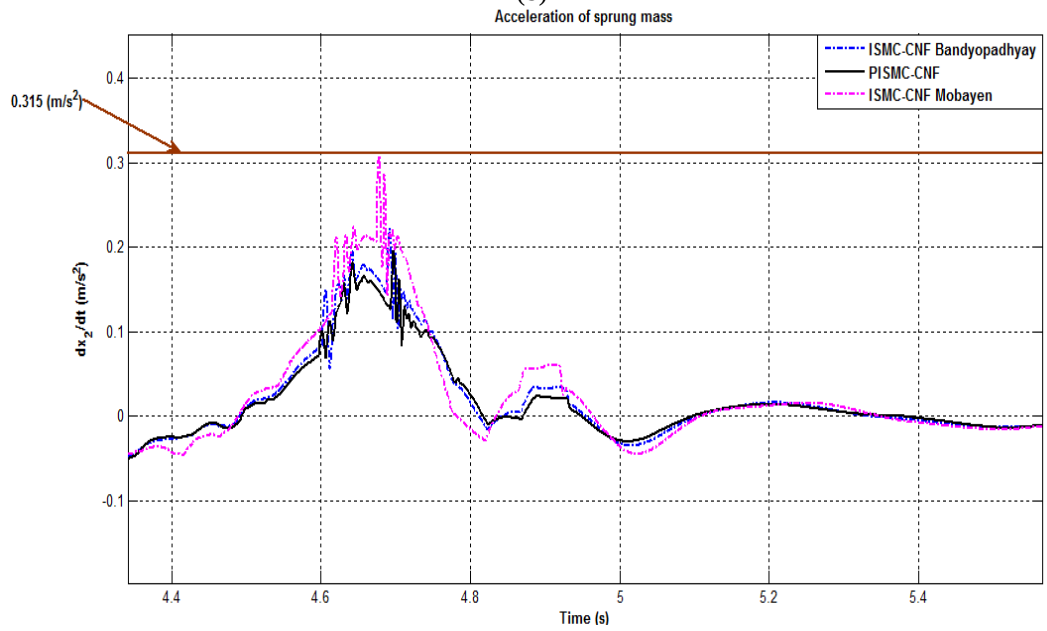

(c)

Figure 9. Acceleration of sprung mass effects for: (a) Bounce sine sweep (b) Chassis twisted and (c) Large smooth bump

5. CONCLUSION

The proposed controller PISMC-CNF has been successfully designed and evaluated for its control performance. The numerical simulation on the control performance showed that the PISMC-CNF was successfully tested under boundary layer thickness and sigmoid function. The chattering suppression has been reduced with a suitable value for boundary layer thickness and sigmoid function by using ES. In future work, the super twisting method is another alternative method to reduce chattering suppression in SMC which is can be applied to the similar system.

ACKNOWLEDGMENT

Special thanks to Universiti Teknologi Malaysia (UTM) for the Research University Grant Vote 05H02, Ministry of Education (MOE) and Universiti Kuala Lumpur (UniKL) for their support of this research works.

REFERENCES

[1] M. S. Fallah, R. Bhat and W. F. Xie, H_∞ robust control of semi-active Macpherson suspension system: New applied design, *Vehicle System Dynamics*, 48(3), 339–360, 2010.

[2] K.-S. Hong, D.-S. Jeon, W.-S. Yoo, H. Sunwoo, S.-Y. Shin, C.-M. Kim and B.-S. Park, A new model and an optimal pole-placement control of the Macpherson suspension system, *SAE Technical Paper*, 1999-01-1331, 1999.

[3] K. Chen and D. G. Beale, Base dynamic parameter estimation of a Macpherson suspension mechanism, *Vehicle System Dynamics*, 39(3), 227–244, 2003.
[4] Y. M. Goh, J. D. Booker and C. A. McMahon, Uncertainty modeling of a suspension unit, *Proceedings of the Institution of Mechanical Engineers, Part D: Journal of Automobile Engineering*, 219(6), 755–771, 2005.
[5] J. Hurel, A. Mandow and A. Garcia-Cerezo, Kinematic and dynamic analysis of the McPherson suspension with a planar quarter-car model, *Vehicle System Dynamics*, 51(9), 1422–1437, 2013.
[6] Y. M. Sam, J. H. S. Osman and M. R. M. Ghani, A class of proportional-integral sliding mode control with application to active suspension system, *Systems and Control Letters*, 51(3–4), 217–223, 2004.
[7] J. Lin and R.-J. Lian, Hybrid self-organizing fuzzy and radial basis-function neural-network controller for active suspension systems, *International Journal of Innovative Computing, Information and Control*, 7(6), 3359–3378, 2011.
[8] A. Chamseddine, H. Noura and T. Raharijaona, Control of linear full vehicle active suspension system using sliding mode techniques. *IEEE International Conference on Control Applications*, Munich, Germany, 2006, pp. 1306–1311.
[9] S. Zhou and S. Zhang, Semi-active control on leaf spring suspension based on SMC, *Chinese Control and Decision Conference*, Xuzhou, China, 2010, pp. 1462–1466.
[10] B.-C. Chen, Y.-H. Shiu and F.-C. Hsieh, Sliding-mode control for semi-active suspension with actuator dynamics, *Vehicle System Dynamics*, 49(1-2), 277–290, 2010.
[11] A. Pati, S. Singh and R. Negi, Sliding mode controller design using PID sliding surface for half car suspension system, *Students Conference on Engineering and Systems*, Allahabad, India, 2014, pp. 1–6.
[12] P. F. Puleston, S. Spurgeon and G. Monsees, Automotive engine speed control: A robust nonlinear control framework, *IEE Proceedings - Control Theory and Applications*, 148(1), 81–87, 2001.
[13] L. Xiaoqiu and S. Yurkovich, Sliding mode control of delayed systems with application to engine idle speed control, *IEEE Transactions on Control Systems Technology*, 9(6), 802–810, 2001.
[14] S. Govindaswamy, T. Floquet and S. K. Spurgeon, Discrete time output feedback sliding mode tracking control for systems with uncertainties, *International Journal of Robust and Nonlinear Control*, 24, 2098–2118, 2013.
[15] H. Alwi and C. Edwards, An adaptive sliding mode differentiator for actuator oscillatory failure case reconstruction, *Automatica*, 49(2), 642–651, 2013.
[16] B. Zhang and W. Lan, Improving transient performance for output regulation problem of linear systems with input saturation, *International Journal of Robust and Nonlinear Control*, 23(10), 1087–1098, 2013.
[17] Z. Lin, M. Pachter and S. Banda, Toward improvement of tracking performance nonlinear feedback for linear systems, *International Journal of Control*, 70(1), 1–11, 1998.
[18] B. M. Chen, T. H. Lee, K. M. Peng and V. Venkataramanan, Composite nonlinear feedback control for linear systems with input saturation: Theory and an application, *IEEE Transactions on Automatic Control*, 48(3), 427–439, 2003.
[19] V. Utkin, J. Guldner and J. Shi, *Sliding mode control in electro-mechanical systems*, CRC Press, 2009.
[20] X. Zhao, M. Kremb and C. Schindler, Assessment of wheel loader vibration on the riding comfort according to ISO standards, *Vehicle System Dynamics*, 51(10), 1548–1567, 2013.
[21] S. Mobayen, V. J. Majd and M. H. Asemani, Selection of nonlinear function in integral sliding mode-based composite nonlinear feedback method for transient improvement of uncertain linear systems, *The 2nd International Conference on Control, Instrumentation and Automation*, Shiraz, Iran, 2011, pp. 513–518.
[22] S. Mobayen and V. J. Majd, Robust tracking control method based on composite nonlinear feedback technique for linear systems with time-varying uncertain parameters and disturbances, *Nonlinear Dynamics*, 70(1), 171–180, 2012.
[23] S. Mobayen and V. J. Majd, Tracker design using composite nonlinear feedback with application to a DC servomotor, *3rd Power Electronics and Drive Systems Technology*, Tehran, Iran, 2012, pp. 435–440.
[24] S. Mobayen, Robust tracking controller for multivariable delayed systems with input saturation via composite nonlinear feedback, *Nonlinear Dynamics*, 76(1), 827–838, 2014.
[25] S. Mobayen, Design of CNF-based nonlinear integral sliding surface for matched uncertain linear systems with multiple state-delays, *Nonlinear Dynamics*, 77(3), 1047–1054, 2014.
[26] B. Bandyopadhyay, D. Fulwani and Y. J. Park, A robust algorithm against actuator saturation using integral sliding mode and composite nonlinear feedback, *Proceedings of the 17th World Congress The International Federation of Automatic Control*, Seoul, South Korea, 2008, pp. 14174–14179.